



# Inferred Immune-Cell Activity Is an Independent Predictor of HER2-Negative Breast Cancer Prognosis and Response to Paclitaxel-Based Therapy in the GeparSepto Trial

Peter A. Fasching<sup>1</sup>, Christopher Szeto<sup>2</sup>, Carsten Denkert<sup>3</sup>, Stephen Benz<sup>2</sup>, Karsten Weber<sup>4</sup>, Patricia Spilman<sup>5</sup>, Jan Budczies<sup>6</sup>, Andreas Schneeweiss<sup>7</sup>, Elmar Stickeler<sup>8</sup>, Sabine Schmatloch<sup>9</sup>, Christian Jackisch<sup>10</sup>, Thomas Karn<sup>11</sup>, Hans Peter Sinn<sup>12</sup>, Mathias Warm<sup>13</sup>, Marion van Mackelenbergh<sup>14</sup>, Shahrooz Rabizadeh<sup>2</sup>, Christian Schem<sup>15</sup>, Ernst Heinmöller<sup>16</sup>, Volkmar Mueller<sup>17</sup>, Frederik Marme<sup>18</sup>, Patrick Soon-Shiong<sup>5</sup>, Valentina Nekljudova<sup>4</sup>, Michael Untch<sup>19</sup>, and Sibylle Loibl<sup>4</sup>

## ABSTRACT

**Purpose:** Tumor microenvironment (TME) immune markers have been correlated with both response to neoadjuvant therapy and prognosis in patients with breast cancer. Here, immune-cell activity of breast cancer tumors was inferred by expression-based analysis to determine if it is prognostic and/or predictive of response to neoadjuvant paclitaxel-based therapy in the GeparSepto (G7) trial (NCT01583426).

**Experimental Design:** Pre-study biopsies from 279 patients with HER2-negative breast cancer in the G7 trial underwent RNA-seq-based profiling of 104 immune-cell-specific genes to assess inferred Immune Cell Activity (iICA) of 23 immune-cell types. Hierarchical clustering was used to classify tumors as iICA “hot,” “warm,” or “cold” by comparison of iICA in the G7 cohort relative to that of 1,467 samples from a tumor database established by Nantomics LLC. Correlations between iICA cluster, pathology-assessed

tumor-infiltrating lymphocytes (TIL), and hormone receptor (HR) status for pathologic complete response (pCR), disease-free survival (DFS), and overall survival (OS) were determined.

**Results:** iICA cluster correlated with TIL levels. The highest pCR rates were observed in hot cluster tumors, and those with relatively higher TILs. Greater inferred activity of several T-cell types was significantly associated with pCR and survival. DFS and OS were prolonged in patients with hot or warm cluster tumors, the latter particularly for HR negative tumors, even if TILs were relatively low.

**Conclusions:** Overall, TIL level better predicted pCR, but iICA cluster better predicted survival. Differences in associations between TILs, cluster, pCR, and survival were observed for HR-positive tumors versus HR-negative tumors, suggesting expanded study of the implication of these findings is warranted.

## Introduction

Immunosurveillance suppression, evasion, and/or avoidance have emerged as key targetable hallmarks of cancer that are driven, in part, by checkpoint expression, T-cell exhaustion, and an immunosuppressive tumor microenvironment (TME; ref. 1). Many of these processes generate defined combinations of immune-cell infiltrates at the tumor site that can be detected by pathology, IHC, CyTOF, or inferred from gene-expression deconvolution (2).

As described previously (3–5), immune profiles that consider tumor-infiltrating lymphocytes (TIL) or lack thereof, as well as expression of other immune cell activity-related genes in the TME, are frequently referred to as either immunologically “hot” or “cold.” Hot tumors show CD8<sup>+</sup> (and other) T-cell infiltration and secretion of chemokines as well as type 1 IFN $\gamma$ , whereas the TME of cold tumors is surrounded by myeloid-derived suppressor cells (MDSC) and T-regulatory cells (Treg) that dampen the immune response (3, 4, 6).

<sup>1</sup>Department of Gynecology and Obstetrics, University Hospital Erlangen, Comprehensive Cancer Center Erlangen-EMN, Friedrich-Alexander University Erlangen-EMN, Erlangen, Germany. <sup>2</sup>Nantomics, LLC, Santa Cruz, California. <sup>3</sup>Institute for Pathology, Philipps University of Marburg, Marburg, Germany. <sup>4</sup>German Breast Group (GBG), Neu Isenburg, Germany. <sup>5</sup>ImmunityBio, Inc., Culver City, California. <sup>6</sup>Institute for Pathology, Heidelberg University Hospital, Heidelberg, Germany. <sup>7</sup>National Center for Tumor Diseases, Heidelberg University Hospital, German Cancer Research Center (DKFZ), Heidelberg, Germany. <sup>8</sup>Department of Gynecology and Obstetrics, University Hospital, RWTH Aachen, Germany. <sup>9</sup>Breast Cancer Center, Elisabeth-Krankenhaus Kassel, Kassel, Germany. <sup>10</sup>Department of Gynecology and Obstetrics, Sana Hospital Offenbach, Offenbach, Germany. <sup>11</sup>Department of Gynecology and Obstetrics, Goethe University Frankfurt, UCT-Frankfurt-Marburg, Frankfurt, Germany. <sup>12</sup>Division of Gynecopathology, Institute for Pathology, University Hospital Heidelberg, Germany. <sup>13</sup>Clinic of the City of Cologne, Cologne, Germany. <sup>14</sup>University Hospital Schleswig-Holstein, Clinic for Gynecology and Obstetrics, Schleswig-Holstein, Germany. <sup>15</sup>Breast Center Hamburg, Hospital Jerusalem, Hamburg, Germany. <sup>16</sup>Institute of Pathology, Pathology Nordhessen, Kassel, Germany. <sup>17</sup>Department of

Gynecology and Obstetrics, University Hospital Hamburg-Eppendorf, Hamburg, Germany. <sup>18</sup>Department of Gynecology and Obstetrics, University Hospital Mannheim, Mannheim, Germany. <sup>19</sup>Helios Hospital Berlin-Buch, Berlin, Germany.

P.A. Fasching and C. Szeto contributed equally to this article.

M. Untch and S. Loibl contributed equally as a senior author to this article.

**Corresponding Author:** Peter Fasching, Department of Gynecology and Obstetrics, University Hospital Erlangen, Comprehensive Cancer Center Erlangen-EMN, Friedrich-Alexander University Erlangen-EMN, Erlangen, Germany. E-mail: Peter.Fasching@UK-Erlangen.de

Clin Cancer Res 2023;XX:XX-XX

doi: 10.1158/1078-0432.CCR-22-2213

This open access article is distributed under the Creative Commons Attribution-NonCommercial-NoDerivatives 4.0 International (CC BY-NC-ND 4.0) license.

©2023 The Authors; Published by the American Association for Cancer Research

## Translational Relevance

Tumor immune profiling, including assessment of tumor-infiltrating lymphocytes (TIL) and expression-based analyses have been reported to be prognostic and predictive of response to a variety of neoadjuvant and immune-based therapies for several cancer types. Here, we expanded such analysis to a subset of patients with HER2-negative breast cancer in the GeparSepto clinical trial wherein solvent-based paclitaxel therapy was compared with nab (albumin)-paclitaxel by application of our developed method for inferred immune cell activity (iICA) assessment and classification of tumors as hot, warm, or cold by hierarchical clustering. Our multivariate analyses of iICA of 23 immune cell types and cluster was found to be independently prognostic, reasonably predictive of response to therapy, and revealed differences in associations for hormone receptor-positive versus negative tumors, suggesting iICA may provide important information for clinical decision-making when paclitaxel-based therapies are being considered.

Baseline, pre-neoadjuvant therapy TME immune profiles comprising TIL level and gene expression—including immune-cell activity inferred from transcriptome assessment—have been correlated with both prognosis in patients with breast cancer and response to chemo- or immune-based therapy (7–20). In a comprehensive analysis, Denkert and colleagues (7) assessed correlation of TILs with chemotherapy response and prognosis in patients from six clinical trials for breast cancer that included triple-negative, HER2-positive, and luminal-HER2-negative breast cancer; and found that the percentage of HER2-negative patients with a pathologic complete response (pCR) increased with an increasing TIL level in response to therapy, but did not find a survival benefit for that subset.

Herein, we investigated the hypothesis that RNA-seq-based inferred Immune Cell Activity (iICA) of breast cancer, comprising both the assessment of relative individual immune-cell activity and clustering of tumors as hot, warm, or cold based on those activities, is predictive of pCR and/or survival in the neoadjuvant GeparSepto (G7) trial (NCT01583426) wherein paclitaxel and nab-paclitaxel therapy were compared (21–24). Paclitaxel has been reported to lead to the induction of TILs (25) and in some cases, suppression of Tregs (14, 26), therefore the relationship between tumor immune profile and response to paclitaxel treatment is of particular interest.

In metastatic breast cancer, solvent-free albumin-encapsulated nab-paclitaxel has been shown to significantly increase progression-free survival (PFS) compared with solvent-based paclitaxel (22) and is associated with lower toxicity (27, 28). The G7 phase III randomized trial assessed whether weekly nab-paclitaxel could increase the proportion of patients achieving pCR compared with weekly solvent-based paclitaxel (21), both followed by epirubicin plus cyclophosphamide as neoadjuvant treatment (29) as recommended by the national guidelines of the AGO-Breast commission (30).

As part of the G7 trial design, biopsies were taken at enrollment before treatment, providing the samples needed to perform RNA-seq-based iICA. In this study, samples from HER2-negative patients underwent the analyses described above.

## Experimental Design

### Patients and treatment

The G7 trial, “Nanoparticle-based Paclitaxel vs. Solvent-based Paclitaxel as Part of Neoadjuvant Chemotherapy for Early Breast Cancer (GeparSepto/NCT01583426),” was a two-arm randomized phase III trial comparing neoadjuvant nab-paclitaxel to solvent-based paclitaxel followed by standard chemotherapy combination of epirubicin and cyclophosphamide in patients with high-risk early-stage breast cancer (21–24). An overview of the trial is shown in Supplementary Fig. S1. Patients were recruited in multiple study sites in Germany. The study was approved by all respective ethic committees (Leading Ethics Committee was in the State of Berlin; 12/0002- ZS EK 13) and all patients gave a written informed consent. The study was conducted in accordance with the Declaration of Helsinki.

Enrolled patients had previously untreated unilateral or bilateral primary invasive breast cancer and were randomly assigned in a 1:1 ratio using dynamic allocation and Pocock minimization by breast cancer subtype, as well as Ki-67 and SPARC expression. Patients were treated for 12 weeks with either intravenous nab-paclitaxel 150 mg/m<sup>2</sup> (after study amendment, 125 mg/m<sup>2</sup>) on days 1, 8, and 15 for four 3-week cycles; or solvent-based intravenous paclitaxel 80 mg/m<sup>2</sup> on days 1, 8, and 15 for four 3-week cycles. Taxane treatment was followed in both groups by intravenous epirubicin 90 mg/m<sup>2</sup> plus intravenous cyclophosphamide 600 mg/m<sup>2</sup> on day 1 for four 3-week cycles.

A total of 1,206 patients received treatment (606 nab-paclitaxel, 600 solvent-based paclitaxel) in the G7 trial; 810 of them were HER2-negative (Supplementary Table S1).

### Pathology and survival assessment

For all patients in the study, breast cancer and hormone receptor (HR; estrogen receptor, ER; progesterone receptor, PR), HER2, Ki-67, and SPARC status were confirmed by central pathology review on core biopsies. In case of bilateral cancer, the investigator decided prospectively which side was to be evaluated for the primary endpoint and the analysis herein, and for patients with multifocal or multicentric breast cancer, the largest lesion was used. Patients were in disease stage cT2–cT4 or cT1c and at least one of the following high-risk conditions: clinical node positive (cN+), non-sentinel lymph node positive (NSLN+) ER-negative, PR-negative, Ki-67 > 20%, or HER2-positive.

IHC-based ER/PR-positive is defined as >1% stained cells and HER2-positive is defined as IHC 3+ or ISH ratio ≥2.0.

Response to treatment included pCR, as assessed by central pathology review. Disease-free survival (DFS) and overall survival (OS) were also assessed in the G7 trial as part of the design.

### RNA-seq-based immune-cell activity assessment

For this study, a retrospective-prospective analysis of the subset of 279 HER2-negative patients in the G7 trial from whom adequate baseline pre-study FFPE biopsy tissue was available for analysis was performed using deep, whole-transcriptome RNA-seq [~200 × 10 (6) reads per tumor] as described previously in Newton and colleagues wherein quality metrics are presented (31).

Immune activity of G7 HER2-negative tumors was inferred by comparison of expression activity associated with 23 immune-cell types at ImmunityBio Inc. using 104 immune-cell specific genes (Supplementary Table S2) described by Bindea and colleagues (2) to those from a reference population of 1,467 similarly-profiled tumor samples (Supplementary Fig. S2) comprising a wide range of tissue types from a large tumor database (Nantomics, LLC; Supplementary

Table S3; ref. 31). The method used for iICA analysis and hierarchical clustering was developed in-house at Nantomics (32).

Additionally for each G7 patient, activity scores of the 23 immune-cell types were categorized being above (high), within, or below (low) one SD (1SD) of the mean of the reference population from the database. These values are referred to as relative immune cell activity categories.

Unsupervised clustering of the relative activities of immune cells as described above was performed, and revealed three major clusters (Fig. 1A) that were then designated as “hot,” “warm,” or “cold.” An unsupervised method is used for clustering because there is no target or outcome variable and relationships between observations are unknown (33). Three clusters was identified as optimal using the elbow method on cluster silhouette coefficients. Each patient sample was assigned an iICA cluster profile.

**TIL scoring**

Biopsies collected as part of the G7 study underwent pathology-based TIL scoring, performed as described in Hendry and colleagues and Salgado and colleagues (34, 35). The units for TILs are percentage of area covered. TILs were analyzed as a continuous measurement and dichotomized at the median to characterize tumors into one of two

groups of similar size—stromal TILs (sTIL) low ( $\leq 15\%$ ) or high ( $>15\%$ ) and similarly, intratumoral TILs (iTIL) low ( $\leq 5\%$ ), or high ( $>5\%$ )—using a method similar to that reported in Denkert and colleagues (7), but with a higher sTIL cutoff ( $\leq 15\%$  rather than  $\leq 10\%$ ), due to the absence of cases with sTILs between 10% and 15%.

**HER2-negative G7 breast cancer analyses**

**Checkpoint expression**

The expression level of checkpoint genes *PDL1*, *CTLA4*, *PDI*, *PDL2*, *LAG3*, *TIGIT*, *OX40*, *FOXP3*, *TIM3*, and *IDO* were assessed and relative levels in hot, warm, and cold iICA clusters determined.

**H&E slide image-based TIL scoring versus CD8 T-cell inferred activity**

The correlation of relative immune cell activity score of CD8<sup>+</sup> T cells and iTILs as scored by standardized methods was determined.

**Individual immune-cell activity score and other variables**

Relative immune cell activity scores in G7 patients with breast cancer in relation to their HR status (triple-negative vs. HR-positive), grade (3 vs. 1–2), and Ki-67 status was also assessed.

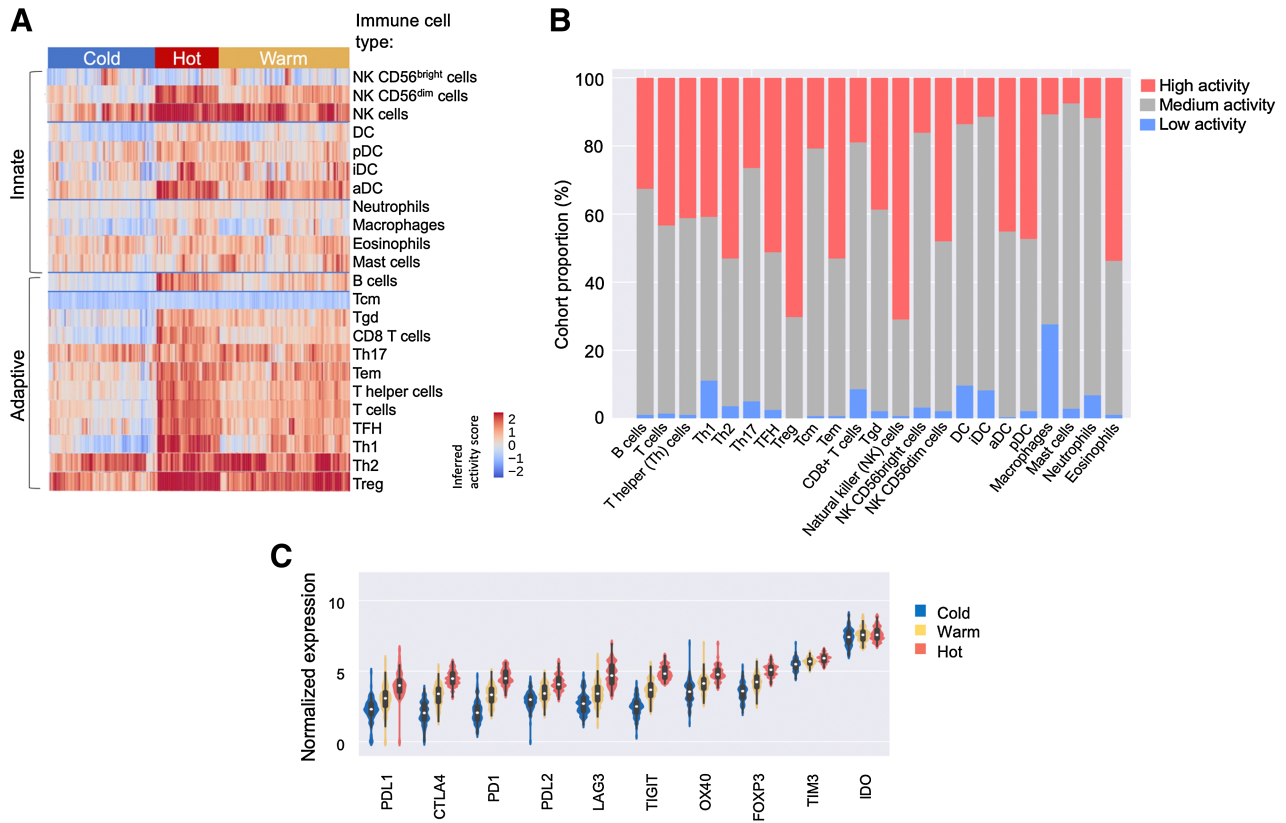


**Figure 1.**

Unsupervised clustering of HER2-negative G7 patient iICA scores reveals three clusters with differential checkpoint expression. **A**, iICA based on relative expression of immune activity-related genes of individual immune-cell subpopulations as compared with breast cancer tumors from the Nantomics tumor database was used to cluster tumor immune signature as cold (blue), hot (red), or warm (yellow). Immune cell types are grouped as part of the innate or adaptive immune response. **B**, The proportion of G7 HER2-negative tumors with relative immune scores that are high (1SD above the mean; red), medium (within 1SD of the mean; grey), or low (less than –1SD of the mean; blue) compared with the reference breast cancer tumors are shown. **C**, Checkpoint gene expression in cold, warm, or hot clusters is shown. Statistics performed using two-sample Wilcoxon tests; differences in checkpoint expression between clusters were significant ( $P < 0.0001$ ) for all checkpoint genes with the exception of IDO.

## Survival

OS and DFS were grouped by iICA clusters and graphed by Kaplan–Meier methods for all HER2-negative patients and those that were HR-positive and HR-negative. Further subgroup clinical variable analyses based on tumor stage, grade, receptor status, metastasis, Ki-67 status, sTILs, iTILs, and study arm (nab-paclitaxel, solvent-based paclitaxel) were also performed.

iICA and pCR: The probability of pCR as determined in the G7 study was analyzed by iICA cluster (hot, warm, cold) and by relative individual immune cell activity scores.

## Statistical considerations

Pairwise comparisons of checkpoint gene expression between clusters were performed using two-sample Wilcoxon tests, and comparisons of all three cluster categories were performed by a Kruskal–Wallis tests.

Prognostication of endpoint pCR defined as ypT0/ypN0 was performed by logistic regression models; prognostication of endpoints DFS and OS was performed by Cox regression. Each regression model contained additional covariables age (continuous), tumor size (T1–2 vs. T3–4), nodal status (N0 vs. N+), HR (TNBC vs. positive), Ki-67 (continuous), and treatment arm (nab-paclitaxel vs. solvent-based paclitaxel). OR (for pCR) and hazard ratios (HR, for DFS and OS) with 95% confidence intervals and corresponding Wald *P* values are reported for immune activity variables and iICA clusters (but not for the covariables).

Tests for interactions between a clinical variable and the iICA cluster were performed by adding the respective terms to the regression model; only interaction *P* values are reported from these models.

Other statistical methods used for comparisons of iICA of 23 immune cell types, iICA cluster, sTILs, and/or HR status for DFS, OS, or pCR are described in Results.

## Availability of data and material

The GeparSepto study protocol, statistical report, and individual participant data are available upon reasonable request to the GBG scientific board <http://www.gbg.de/de/forshung/translacionale-forshung.php>. The iICA data are available upon reasonable request to [info@nanotomics.com](mailto:info@nanotomics.com).

The gene expression data files are accessible via the Sequence Read Archive (SRA): <https://www.ncbi.nlm.nih.gov/sra?term=PRJNA944217>

# Results

## Patient characteristics

Demographics and patient tumor status (grade, receptor expression, etc.) are shown in Supplementary Table S1. Of the 279 patients, 67 had a pCR (24%); this was similar to the total G7 HER2-negative population pCR rate (22%) that included patients for whom sufficient baseline biopsy tissue was not available for analysis and those whose samples failed RNA-seq QC criteria. In the analyzed subset, 73.5% were also HR-positive whereas in the total HER2-negative population, it was 65.9%.

## G7 HER2-negative BC patient iICA hot, warm, and cold clusters

The hot, warm and cold clusters (*n* = 58, 121, and 100, respectively) established from G7 HER2-negative BC patient biopsy iICA data (36, 37) are shown in Fig. 1A. In the cold cluster, adaptive immune cell types such as natural killer (NK) CD56 dim and CD8+ T cells were inferred to be inactive/low activity while Th2 and Treg activity was present. In the hot cluster, adaptive immune-cell activity is

higher than that in the warm cluster, particularly for NK cells, activated DCs (aDCs), and almost all T-cell types, including Tregs. While Th2 activity is increased in the cluster, Th1 activity shows a distinct increase as well, resulting in a relatively higher Th1/Th2 ratio (Supplementary Fig. S3). Warm is distinguished by having lower NK, DC, B-cell and anti-tumor T-cell activity than the hot cluster (but not as low as the cold cluster) and while there is an increase in Treg and Th2 activity, it is not seen with the same level of increase in Th1 activity as seen in the hot cluster.

The proportion of patients with a high, medium, or low relative immune cell activity score for each of the 23 cell types is shown in Fig. 1B. The cell types for which the greatest proportion of the G7 HER2-negative breast cancer cohort were assessed to have high activity were NK cells (71.0%) and Tregs (70.3%). Stimulatory T-cell signatures were high in approximately half of the G7 HER2-negative cohort including Th2 cells (53.0%), effector-memory (Tem; 53.0%), T follicular helper (TFH) cells (51.3%), Th1 cells (40.9%), and  $\gamma$ -delta T cells (Tgd; 38.7%). Although cytotoxic CD8+ T-cell signature was high in only 19.0% of the cohort, the signature for the CD56dim cytolytic subset of NK cells was high in 48.0% of patients. Innate immune-response cell types with high activity comprised the smallest proportion of the cohort and included mast cells (7.5%), macrophages (10.8%), iDCs (11.5%), and neutrophils (11.8%).

The expression of immune checkpoint genes was greatest in the hot cluster, lowest in the cold cluster, and intermediate in the warm cluster; differences between clusters were highly significant, with the exception of IDO (Fig. 1C; Supplementary Table S4).

## Correlation between iICA and TIL scoring

RNA-seq-based deconvolution of immune-cell activity was corroborated by TIL scoring using H&E stained tissue biopsy sections (38). As shown in Fig. 2A and B, levels of both stromal TILs (sTIL) and intratumoral TILs (iTIL) as determined by conventional scoring are lowest in the cold cluster, intermediate in the warm cluster, and highest in the hot cluster (Fig. 2B).

The iICA score of CD8+ T cells specifically correlates with iTIL level (Fig. 2C). CD56dim NK and Th1 cells were also moderately correlated with the percentage of iTILs, with Spearman correlation coefficients of 0.461 and 0.525, respectively.

## Immune-cell activity associated with HR status, grade, and Ki-67 expression

Of the 279 HER2-negative patients, 74 were triple negative (TNBC), that is, HR-negative as well as HER2-negative, and 205 were HR-positive (Supplementary Table S1). In TNBC, the inferred activities of Th1, Tregs, NK CD56dim cells, dendritic cells (DC), aDCs, and macrophages were significantly higher as compared with HR-positive tumors; whereas in HR-positive breast cancer in the cohort, inferred activities of Th2 and NK CD56bright were significantly higher (Supplementary Fig. S4A). When grade 3 tumors (*n* = 162) were compared with grade 1 to 2 tumors (*n* = 117), B cells, Th1, Tregs, NK CD56dim cells, and aDCs were significantly higher. In grade 1 to 2 tumors, Th2, T helper type 17 (Th17) cells, mast cells, and NK CD56bright cells were significantly higher compared with grade 3 (Supplementary Fig. S4B). There were many positive correlations to Ki-67 expression, including B cells, T cells, helper T cells, Th1, TFH, Tregs, CD8+ T cells, NK CD56dim cells, DCs, aDCs, and macrophages; Th2, Th17, NK CD56bright cells, eosinophils, iDCs, plasmacytoid DCs (pDC), and mast cells were negatively correlated with Ki-67 expression (Supplementary Fig. S4C).

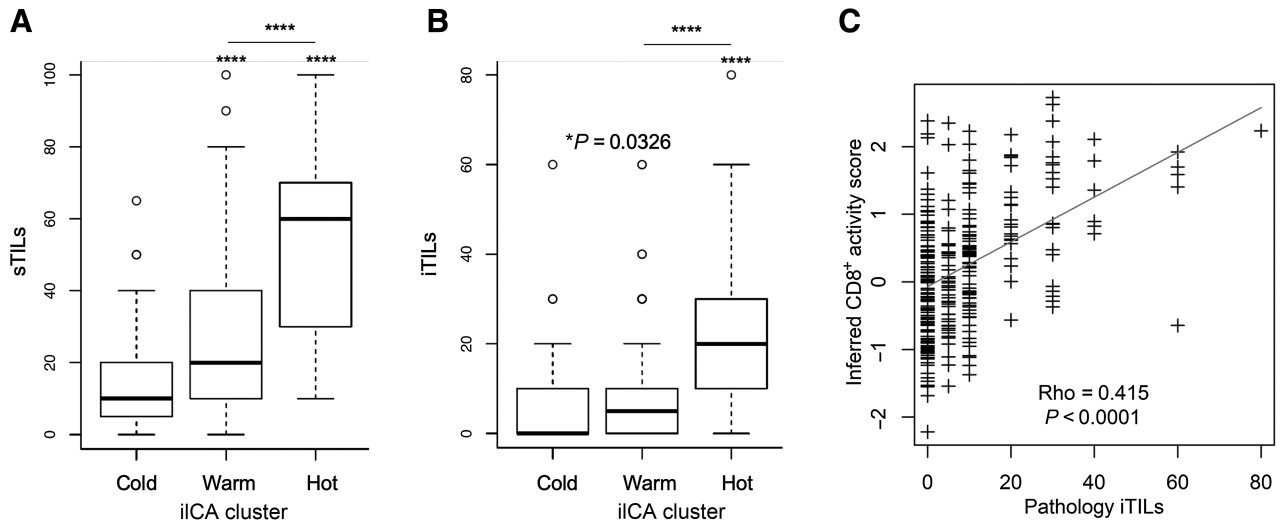


**Figure 2.**

RNA-seq-based immune-cell deconvolution correlates with TIL scoring. The level of (A) sTILs and (B) iTILs as detected by pathology-based TIL scoring correlates with iICA cluster, with TIL numbers being greater in the warm than the cold cluster, and highest in the hot cluster. Statistics performed using two-sample Wilcoxon test, where \*\*\*\* $P < 0.0001$  and \* $P \leq 0.05$  (\* $P$ -value shown); cold  $n = 100$ , warm  $n = 121$ , and hot  $n = 58$ . C, Comparison of inferred CD8<sup>+</sup> activity score (y-axis) and iTILs (x-axis) also reveals a highly significant correlation ( $P < 0.001$ ) and a Spearman correlation coefficient of 0.415. The gray line represents a linear regression model.

**Individual iICA score and pCR rate**

Higher inferred activities of B cells, CD8<sup>+</sup> T cells, DCs, Th cells, macrophages, natural killer (NK) CD56dim cells, T cells, Th1 cells, Tregs, aDCs, and TFH cells were found to be closely correlated with pCR (Supplementary Fig. S5). Inferred increases in NK, neutrophil, T central memory (T<sub>cm</sub>), T effector memory (T<sub>em</sub>), and T gamma delta (T<sub>gd</sub>) activities were also associated with pCR. Decreased inferred eosinophil, Th2, and NK CD56bright cell activity was associated with pCR. Only inferred mast cell, Th17, iDC, and pDC activities were not associated with pCR.

Additional analyses of the correlation of specific immune cell inferred activity and pCR were performed. Of the 23 immune-cell types, higher TFH cell inferred activity was most closely correlated with a higher pCR rate (Supplementary Fig. S6A). Inferred TFH activity was also associated with OS and DFS (Supplementary Fig. S6B), with multivariable Cox regression analysis showing a highly significant association. In similar multivariate analyses, B cells, CD8<sup>+</sup> T cells, helper T cells, mast cells, T cells, Tgd, Th1, and Th2 (all HRs <1 and  $P$  values <0.05) also predicted DFS and OS.

**Patients in the hot cluster have the highest pCR rate**

The pCR rate for cold, warm, and hot cluster G7 HER2-negative patients was 13.0%, 21.5%, and 48.3%, respectively (Fig. 3A; Supplementary Table S5). The pCR rate was also highest for the hot cluster for both HR-positive and -negative patients, although the differences among clusters were less for the HR-negative group (Supplementary Table S5). This may have been due to iICA cluster having a lesser influence in HR-negative patients.

For pCR, there were no statistically (Fisher exact test) significant differences between the cold and warm iICA clusters regardless of HR status (Supplementary Table S6), but the difference between the cold and hot clusters was highly significant for all patients, driven by the HR-positive.

**pCR, cluster, sTILs, and HR status**

As shown in Fig. 3A, most patient biopsies in the cold cluster had  $\leq 15\%$  sTILs and those in the warm and hot clusters had  $>15\%$  sTILs. The highest percentage of patients with a pCR was observed in the hot cluster with  $>15\%$  sTILs.

Overall, a higher pCR rate of 50.0% was achieved in HR-negative (neg) versus 14.6% in HR-positive (pos) patients (Fig. 3B and C; Supplementary Table S7). The pCR rates in HR-negative patients with sTILs  $\leq 15\%$  or  $>15\%$  were 35.0% or 55.6%, respectively. Within the HR-positive patients those with sTILs  $>15\%$  had a higher pCR rate compared with sTILs  $\leq 15\%$  (23.5% vs. 5.8%).

**iICA cluster independently predicts DFS in subgroups**

Multivariable Cox regression models were calculated in subgroups by known clinical prognostic factors (Fig. 4). No significant interaction between the cluster and a clinical factor with respect to DFS was found; the HRs for the cluster do not differ significantly in subgroups. For this binary analysis, the hot and warm clusters were considered together versus the cold cluster.

**Subjects in distinct immune clusters have differential survival**

Subjects clustered as immune warm had prolonged DFS compared with the cold cluster, and there was a trend toward prolonged DFS in the hot as compared with the cold cluster (Fig. 5A). DFS for HR-positive patients (Fig. 5B) was similar to that for all patients, but for HR-negative patients the hot cluster was intermediate between the warm and cold clusters (Fig. 5C) but not significantly different based on log-rank tests (Supplementary Table S8).

OS was prolonged in the warm and hot clusters as compared with the cold cluster when all or HR pos patients were considered, whereas OS in the hot cluster was more similar to that of the cold cluster for HR-negative patients (Fig. 5D–F, respectively).

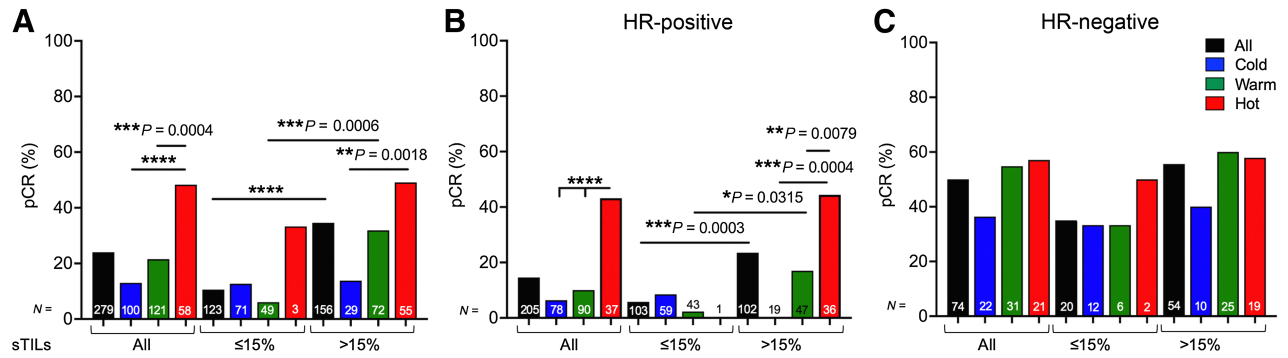


**Figure 3.** pCR, iICA cluster, sTILs, and HR status. The percentage of patients with a pCR is shown for all, sTILs ≤15% and >15% for (A) cold (blue), warm (green) and hot (red) clusters and by HR status (B) positive (pos) and (C) negative (neg). The C applies to A and B; total patient numbers for each group are shown at the bottom of each bar.

**Survival, cluster, sTILs, and iTILs**

As shown in Fig. 6A and B, prolonged DFS was observed for patients in the warm cluster with sTILs ≤15% and/or iTILs ≤5%, followed by patients in the hot cluster with sTILs >15% and/or iTILs >5%. The shortest duration of DFS was observed for cold cluster patients with sTILs either > or ≤15% and iTILs ≤5%. Although it appears that duration of DFS was relatively short for hot cluster patients with sTILs ≤15% and iTILs ≤5%, there were very few of these patients.

The findings for OS (Fig. 6C and D) were similar, with warm cluster patients with sTILs ≤15% and iTILs ≤5% having prolonged OS, and cold cluster patients with sTILs ≤15% and iTILs ≤5% having relatively shorter OS.

**Discussion**

The findings of this study provide evidence that whole-transcriptome sequencing in breast cancer FFPE core biopsies from clinical cohorts used to quantify relative activity of immune cell types can be used in conjunction with conventional pathology-based TIL scoring to predict response to and prognosis after neoadjuvant taxane chemotherapy in early HER2-negative high-risk breast cancer.

The iICA method used was established in-house at Nantomics. To make the relative immune activity meaningful and unbiased, the reference population not only comprised a high number of cases (1,467) but a very broad range of cancer tissue types (Supplementary Table S3). With further development and more widespread

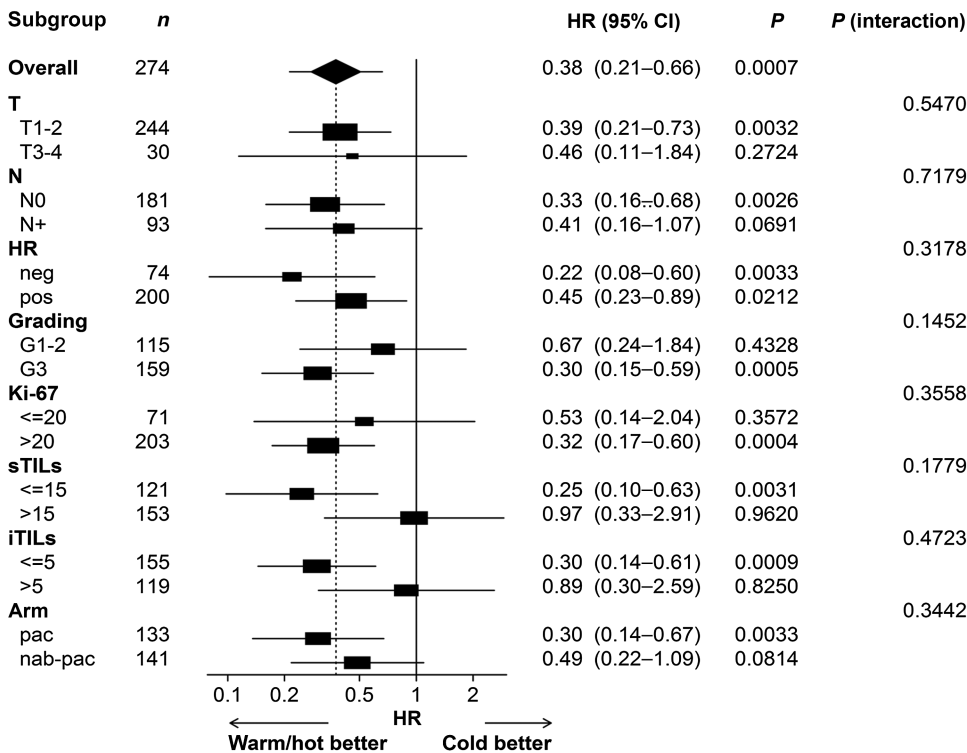


**Figure 4.** Inferred immune cell activity clusters independently predict DFS. Multivariable Cox regression models for DFS in subgroups by other prognostic factors such as stage (T), metastasis/nodal status (N), HR status, grading (G1–G2, G3), Ki-67 expression by IHC, sTILs/iTILs by scoring, and arm of the study (nab-paclitaxel vs. solvent-based paclitaxel).

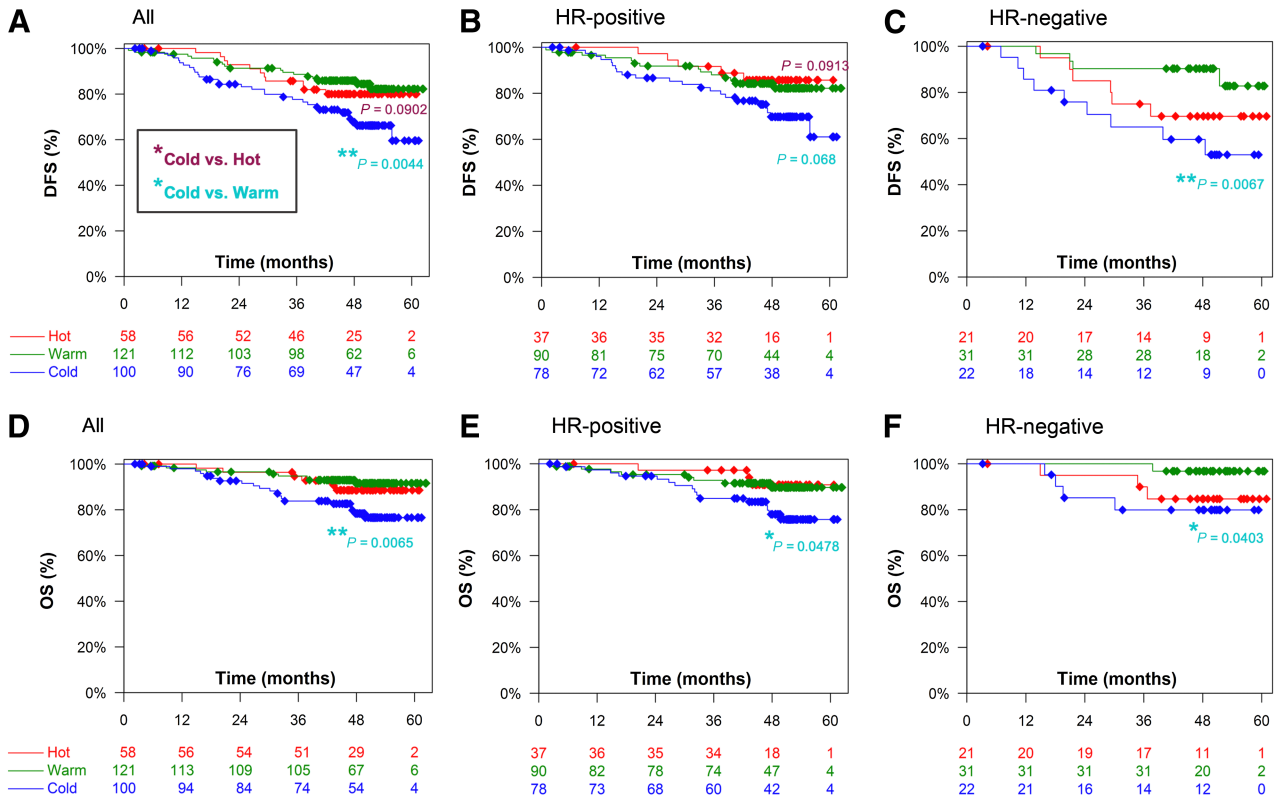


**Figure 5.** Warm and hot clusters have prolonged DFS and OS. DFS for (A) all, (B) HR-positive, and (C) HR negative patients clustered as immune hot (red), warm (green), or cold (blue) is shown. OS for (D) all, (E) HR positive, and (F) HR-negative patients clustered as described in A is shown. Statistical analysis performed using a log-rank test to compare the cold cluster to warm or hot clusters where  $P$  values  $\leq 0.1$  (trend) are shown,  $*P \leq 0.05$ ,  $**P < 0.01$  (additional  $P$  values are listed in Supplementary Table S8). The color code for statistics in A applies to all panels; no significant differences were observed between the warm and hot clusters.

application, it may be desirable for a standard reference database be established for use by investigators so that the designations of cold, warm, or hot (or even additional clusters, as more is revealed about this method) can be standardized across studies.

To more efficiently assess iICA, the method may be refined by use of a panel of 104 genes and NGS. Conversely, the analysis may be expanded to consider the iICA profile along with expression of genes not identified to be directly implicated in the activity of the 23 immune cell types described here. Although this might be considered broad RNA-seq-based tumor characterization, it might be informative in the case of (for example) patients who are immune hot/relatively high TILs who did not respond to therapy to identify factors beyond iICA that alter outcomes.

In the iICA clusters described herein, the warm cluster should not be considered as merely intermediate between hot and cold for the activity of all or most immune-cell types. It is distinguished from the cold cluster by its relatively higher NK and aDC activity, as well as—generally—activity of most T-cell types. The activity of those cell types is further increased in the hot cluster, but with a notable increase in Treg and Th1 activity. The higher activity of Tregs in the hot cluster may seem counter-intuitive if this cluster is considered the most immune-active cluster, but co-upregulation of Tregs (and checkpoint genes) in the presence of both an innate and adaptive immune response may explain tumor immune escape. Higher checkpoint expression in an apparently immune-active environment also supports the greater efficacy of immune-based therapy such as PDL-1 inhibitors

in patients with hot tumors with high tumor TIL scores—immune cells are ready to exert their antitumor effects when the checkpoint molecule is inhibited.

iICA hot tumors also display greater Th1 activity, which likely results in a Th1/Th2 ratio that is favorable, even in the presence of high Th2 activity (Supplementary Fig. S3).

In the cohorts analyzed herein, there was a lesser association of cluster and sTIL level on the pCR rate in HR-negative tumors; patients in the warm cluster with HR-negative tumors had relatively prolonged survival (although the difference from the hot cluster was not statistically significant). Although these data may be due to statistics not being similarly powered in the HR-negative and -positive groups (patient numbers in the HR neg groups were lower), we propose that the higher Treg activity in HR-negative iICA hot cluster tumors resulted in an insignificant difference in the pCR rate as compared with warm cluster tumors and survival that was apparently prolonged in the warm cluster. Such as association in HR-negative breast cancer has previously been reported by Oshi and colleagues (39), who observed a lower response to therapy for high Treg TNBC tumors. Further investigation, including analyses of other cohorts, is necessary to confirm this finding.

iICA profiling has the potential to provide richer and more detailed information on the immune character of tumors than TIL scoring alone. With further development and broader use for analysis of other tumor types and therapies, this method may emerge as an important tool to inform therapeutic decision-making and reveal the

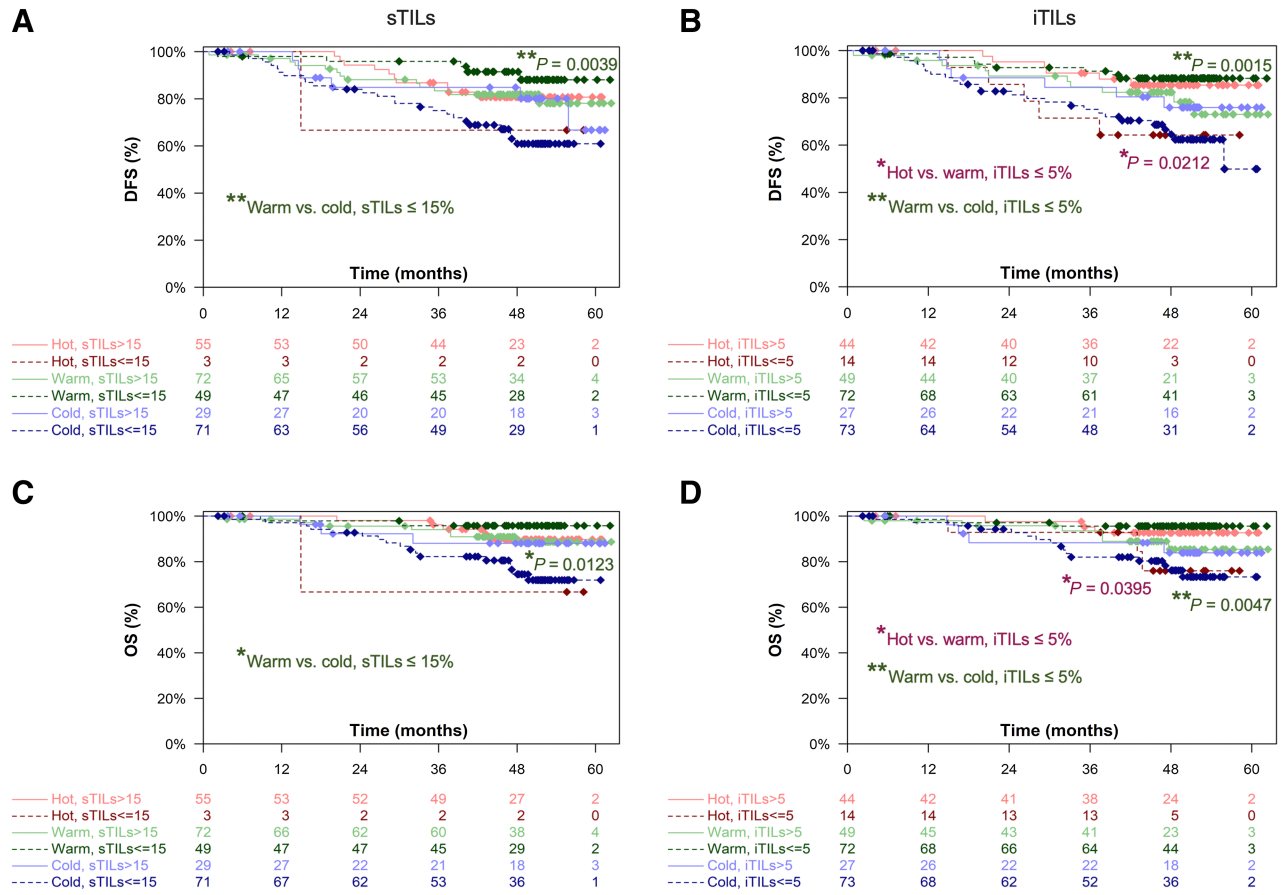


**Figure 6.** Warm cluster patients with sTILs ≤15% or iTILs ≤5% have the longest DFS and OS. DFS based on cluster and (A) sTILs and (B) iTILs; OS based on cluster and (C) sTILs and (D) iTILs are shown. Wald *P* values are from Cox regression models with interaction between cluster and TILs (Supplementary Table S9).

immunobiology of tumors that affects response to therapy and survival.

**Declarations**

**Ethics Approval and Consent to Participate**

The study, including collection and analysis of samples, was approved by all respective ethic committees; the Leading Ethics Committee was in the State of Berlin; 12/0002- ZS EK 13. The study was conducted in accordance with the Declaration of Helsinki. All patients gave a written informed consent.

**Consent for Publication**

Patient consent for publication obtained.

**Authors' Disclosures**

P.A. Fasching reports grants and personal fees from Novartis, Biontech, and Pfizer; personal fees from Daiichi-Sankyo, AstraZeneca, Eisai, Merck Sharp & Dohme, Cepheid, Lilly, Pierre Fabre, Seagen, Roche, Agendia, Sanofi Aventis, and Gilead outside the submitted work. C.W. Szeto reports a patent for WO2019183121A1 pending. C. Denkert reports grants from German Breast Group during the conduct of the study; personal fees from AstraZeneca, Daiichi Sankyo, Lilly, Molecular Health, MSD Oncology, and Roche; other support from Sividon Diagnostics; and grants from Myriad outside the submitted work; also has a patent for Patent applications WO2015114146A1 and WO2010076322A1 issued and a patent for Patent application WO2020109570A1 issued. S.C. Benz reports employment with ImmunityBio, Inc.

and a shareholder in NantOmics, LLC. K. Weber reports grants from BMS during the conduct of the study; grants from Abbvie and AstraZeneca; grants and nonfinancial support from Daiichi-Sankyo, Gilead, Novartis, Pfizer, and Roche; nonfinancial support from Seagen outside the submitted work; also has a patent for EP14153692.0 issued to GBG Forschungs GmbH, a patent for EP21152186.9 issued to GBG Forschungs GmbH, a patent for EP15702464.7 issued to GBG Forschungs GmbH, a patent for EP19808852.8 issued to GBG Forschungs GmbH, and a patent for VM Scope GmbH with royalties paid from GBG Forschungs GmbH; and reports employment with GBG Forschungs GmbH. J. Budczies reports grants from German Cancer Aid and personal fees from MSD outside the submitted work. C. Jackisch reports personal fees from Roche, Celgene, Pfizer, and AstraZeneca during the conduct of the study. T. Karn reports a patent for EP18209672 pending. M.T. van Mackelenbergh reports personal fees from Amgen, Astra Zeneca, GenomicHealth, Gilead, GSK, Lilly, Molecular Health, Mylan, Novartis, Pfizer, PierreFabre, Roche, and Seagen; personal fees and other support from Daiichi Sankyo outside the submitted work. S. Rabizadeh reports employment with Immunity Bio, Inc. and NantBio, Inc. and NantOmics, LLC; receives equity from Immunity Bio as part of my compensation. V. Mueller reports personal fees from speaker honoraria from Amgen, Astra Zeneca, Daiichi-Sankyo, Eisai, GSK, Pfizer, MSD, Medac, Novartis, Roche, Teva, Seagen, Onkowissen, high5 Oncology, Medscape, Gilead, Pierre Fabre Consultancy honoraria from Hexal, Roche, Pierre Fabre, Amgen, ClinSol, Novartis, MSD, Daiichi-Sankyo, Eisai, Lilly, Sanofi, Seagen, and Gilead outside the submitted work. F. Marme reports personal fees from GSK, Roche, Novartis, AstraZeneca, MSD, Vaccibody, Gilead Sciences, Eisai, Pfizer, Myriad, GenomicHealth, Seagen, Daiichi Sankyo, Pierre Fabre, Agendia, Lilly, and Clovis outside the submitted work. P. Soon-Shiong reports other support from NantOmics during the conduct of the study; other support from NantOmics outside the submitted work. V. Nekljudova reports grants from BMS and grants and nonfinancial support from Roche during the conduct of the study; grants



from Abbvie and AstraZeneca; grants and nonfinancial support from Daiichi-Sankyo, Gilead, Novartis, and Pfizer; and nonfinancial support from Seagen outside the submitted work; also has a patent for EP14153692.0 licensed to GBG, a patent for EP21152186.9 licensed to GBG, a patent for EP15702464.7 licensed to GBG, and a patent for EP19808852.8 licensed to GBG. M. Untch reports personal fees from Celgene, Amgen, Astra Zeneca, Daiichi Sankyo, Lilly, MSD Merck, Myriad, Pfizer, Roche, Sanofi Aventis, Novartis, Pierre Fabre, Seagen, and Gilead outside the submitted work. S. Loibl reports grants, nonfinancial support, and other support from Celgene/BMS during the conduct of the study; grants and other support from Abbvie; grants, nonfinancial support, and other support from Amgen, AZ, Pfizer, and Roche; other support from Eirgenix, GSK, Lilly, Merck kGA, Pierre Fabre, Seagen, and Medscape; and grants, nonfinancial support, and other support from Daichi-Sankyo outside the submitted work; also has a patent for VM Scope GmbH with royalties paid, a patent for EP14153692.0 pending, a patent for EP21152186.9 pending, and a patent for EP15702464.7 pending. No disclosures were reported by the other authors.

## Authors' Contributions

**P.A. Fasching:** Visualization, writing—original draft, project administration, writing—review and editing. **C. Szeto:** Conceptualization, formal analysis, investigation, visualization, methodology, writing—original draft, writing—review and editing. **C. Denkert:** Conceptualization, resources, data curation, formal analysis, investigation, visualization, methodology, writing—original draft, writing—review and editing. **S. Benz:** Conceptualization, resources, data curation, supervision, investigation, project administration, writing—review and editing. **K. Weber:** Conceptualization, formal analysis, supervision, investigation, methodology, writing—original draft, writing—review and editing. **P. Spilman:** Formal analysis, investigation, visualization, methodology, writing—original draft, writing—review and editing. **J. Budczies:** Conceptualization, formal analysis, validation, writing—review and editing. **A. Schneeweiss:** Conceptualization, investigation, writing—review and editing. **E. Sticker:** Conceptualization, formal analysis, validation, writing—review and editing. **S. Schmatloch:** Conceptualization, investigation, writing—review and editing.

**C. Jackisch:** Conceptualization, investigation, writing—review and editing. **T. Karn:** Investigation, writing—review and editing. **H.P. Sinn:** Formal analysis, investigation, writing—review and editing. **M. Warm:** Conceptualization, formal analysis, writing—review and editing. **M. van Mackelenbergh:** Investigation, writing—review and editing. **S. Rabizadeh:** Conceptualization, resources, project administration, writing—review and editing. **C. Schem:** Investigation, writing—review and editing. **E. Heinmöeller:** Formal analysis, writing—review and editing. **V. Mueller:** Formal analysis, writing—review and editing. **F. Marmé:** Investigation, writing—review and editing. **P. Soon-Shiong:** Resources, supervision, writing—review and editing. **V. Nekljudova:** Investigation, writing—review and editing. **M. Untch:** Formal analysis, investigation, writing—review and editing. **S. Loibl:** Conceptualization, resources, supervision, funding acquisition, project administration, writing—review and editing.

## Acknowledgments

The G7 study was funded by Celgene and Roche; the iICA analysis was funded by Nantomics, LLC. We thank all patients and their families participating in the G7 trial and the team at the German Breast Group (GBG) Headquarters. We further thank J. Zachary Sanborn at ImmunityBio/NantHealth for data preparation and technical support.

The publication costs of this article were defrayed in part by the payment of publication fees. Therefore, and solely to indicate this fact, this article is hereby marked “advertisement” in accordance with 18 USC section 1734.

## Note

Supplementary data for this article are available at Clinical Cancer Research Online (<http://clincancerres.aacrjournals.org/>).

Received July 21, 2022; revised September 13, 2022; accepted March 31, 2023; published first April 4, 2023.

## References

- Dunn GP, Bruce AT, Ikeda H, Old LJ, Schreiber RD. Cancer immunotherapy: from immunosurveillance to tumor escape. *Nat Immunol* 2002;3:991–8.
- Bindea G, Mlecnik B, Tosolini M, Kirilovsky A, Waldner M, Obenauf AC, et al. Spatiotemporal dynamics of intratumoral immune cells reveal the immune landscape in human cancer. *Immunity* 2013;39:782–95.
- Gajewski TF, Corrales L, Williams J, Horton B, Sivan A, Spranger S. Cancer immunotherapy targets based on understanding the T cell-inflamed versus non-T cell-inflamed tumor microenvironment. *Adv Exp Med Biol* 2017;1036:19–31.
- Galon J, Bruni D. Approaches to treat immune hot, altered and cold tumours with combination immunotherapies. *Nat. Rev. Drug Discov.* 2019;18:197–218.
- Galon Jérôme, Costes A, Sanchez-Cabo F, Kirilovsky A, Mlecnik B, Lagorce-Pagès C, et al. Type, density, and location of immune cells within human colorectal tumors predict clinical outcome. *Science* 2006;313:1960–4.
- De Guillebon E, Dardenne A, Saldmann A, Séguier S, Tran T, Paolini L, et al. Beyond the concept of cold and hot tumors for the development of novel predictive biomarkers and the rational design of immunotherapy combination. *Int. J. Cancer.* 2020;147:1509–18.
- Denkert C, von Minckwitz G, Darb-Esfahani S, Lederer B, Heppner BI, Weber KE, et al. Tumour-infiltrating lymphocytes and prognosis in different subtypes of breast cancer: a pooled analysis of 3771 patients treated with neoadjuvant therapy. *Lancet. Oncol.* 2018;19:40–50.
- Gao Z-h Li C-x Liu M, Jiang J-y. Predictive and prognostic role of tumour-infiltrating lymphocytes in breast cancer patients with different molecular subtypes: a meta-analysis. *BMC Cancer* 2020;20:1150.
- Stanton SE, Disis ML. Clinical significance of tumor-infiltrating lymphocytes in breast cancer. *J. Immunother. Cancer.* 2016;4:59–66.
- Foukakis T, Lötvrot J, Matikas A, Zerdas I, Lorent J, Tobin N, et al. Immune gene expression and response to chemotherapy in advanced breast cancer. *Br. J. Cancer.* 2018;118:480–8.
- Bertucci F, Boudin L, Finetti P, Van Berckelaer C, Van Dam P, Dirix L, et al. Immune landscape of inflammatory breast cancer suggests vulnerability to immune checkpoint inhibitors. *Oncoimmunology* 2021;10:1929724.
- Bedognetti D, Hendrickx W, Marincola FM, Miller LD. Prognostic and predictive immune gene signatures in breast cancer. *Curr Opin Oncol* 2015;27:433–44.
- Sota Y, Naoi Y, Tsunashima R, Kagara N, Shimazu K, Maruyama N, et al. Construction of novel immune-related signature for prediction of pathological complete response to neoadjuvant chemotherapy in human breast cancer. *Ann Oncol* 2014;25:100–6.
- Chaudhary B, Elkord E. Regulatory T cells in the tumor microenvironment and cancer progression: Role and therapeutic targeting. *Vaccines* 2016; 4:28–53.
- Loi S, Sirtaine N, Piette F, Salgado R, Viale G, Van Eenoo F, et al. Prognostic and predictive value of tumor-infiltrating lymphocytes in a phase III randomized adjuvant breast cancer trial in node-positive breast cancer comparing the addition of docetaxel to doxorubicin with doxorubicin-based chemotherapy: BIG 02–98. *J Clin Oncol* 2013;31:860–7.
- Denkert C, Loibl S, Noske A, Roller M, Müller BM, Komor M, et al. Tumor-associated lymphocytes as an independent predictor of response to neoadjuvant chemotherapy in breast cancer. *J Clin Oncol* 2010;28:105–13.
- Ji F, Yuan J-M, Gao H-F, Xu A-Q, Yang Z, Yang C-Q, et al. Tumor microenvironment characterization in breast cancer identifies prognostic and neoadjuvant chemotherapy relevant signatures. *Front Mol Biosci* 2021;8:759495.
- Yam C, Yen E-Y, Chang JT, Bassett RL, Alatrash G, Garber H, et al. Immune phenotype and response to neoadjuvant therapy in triple-negative breast cancer. *Clin Cancer Res* 2021;27:5365–75.
- Ali HR, Chlon L, Pharoah PDP, Markowitz F, Caldas C. Patterns of immune infiltration in breast cancer and their clinical implications: a gene-expression-based retrospective study. *PLoS Med* 2016;13:e1002194.
- Li X, Warren S, Pelekanou V, Wali V, Cesano A, Liu M, et al. Immune profiling of pre- and post-treatment breast cancer tissues from the SWOG S0800 neoadjuvant trial. *J Immunother Cancer* 2019;7:88–97.
- Untch M, Jackisch C, Schneeweiss A, Conrad B, Aktas B, Denkert C, et al. Nab-paclitaxel versus solvent-based paclitaxel in neoadjuvant chemotherapy for early breast cancer (GeparSepto-GBG 69): a randomised, phase 3 trial. *Lancet. Oncol.* 2016;17:345–56.
- Untch M, Jackisch C, Schneeweiss A, Schmatloch S, Aktas B, Denkert C, et al. NAB-paclitaxel improves disease-free survival in early breast cancer: GBG 69-GeparSepto. *J Clin Oncol* 2019;37:2226–34.

23. Loibl S, Jackisch C, Schneeweiss A, Schmatloch S, Aktas B, Denkert C, et al. Dual HER2-blockade with pertuzumab and trastuzumab in HER2-positive early breast cancer: a subanalysis of data from the randomized phase III GeparSepto trial. *Ann Oncol* 2017;28:497–504.
24. Furlanetto J, Jackisch C, Untch M, Schneeweiss A, Schmatloch S, Aktas B, et al. Efficacy and safety of nab-paclitaxel 125 mg/m<sup>2</sup> and nab-paclitaxel 150 mg/m<sup>2</sup> compared to paclitaxel in early high-risk breast cancer. Results from the neoadjuvant randomized GeparSepto study (GBG 69). *Breast Cancer Res Treat* 2017;163:495–506.
25. Demaria S, Volm MD, Shapiro RL, Yee HT, Oratz R, Formenti SC, et al. Development of tumor-infiltrating lymphocytes in breast cancer after neoadjuvant paclitaxel chemotherapy. *Clin Cancer Res* 2001;7:3025–30.
26. Chen C, Chen Z, Chen D, Zhang B, Wang Z, Le H. Suppressive effects of gemcitabine plus cisplatin chemotherapy on regulatory T cells in non-small-cell lung cancer. *J Int Med Res* 2015;43:180–7.
27. Gardner ER, Dahut WL, Scripture CD, Jones J, Aragon-Ching JB, Desai N, et al. Randomized crossover pharmacokinetic study of solvent-based paclitaxel and nab-paclitaxel. *Clin Cancer Res* 2008;14:4200–5.
28. Vishnu P, Roy V. Safety and efficacy of nab-paclitaxel in the treatment of patients with breast cancer. *Breast Cancer* 2011;5:53–65.
29. Anampa J, Makower D, Sparano JA. Progress in adjuvant chemotherapy for breast cancer: an overview. *BMC medicine* 2015;13:195–.
30. Liedtke C, Jackisch C, Thill M, Thomssen C, Müller V, Janni W. AGO recommendations for the diagnosis and treatment of patients with early breast cancer: Update 2018. *Breast Care* 2018;13:196–208.
31. Newton Y, Sedgewick AJ, Cisneros L, Golovato J, Johnson M, Szeto CW, et al. Large scale, robust, and accurate whole transcriptome profiling from clinical formalin-fixed paraffin-embedded samples. *Sci Rep* 2020;10:17597.
32. Szeto C, Reddy S. Immune Cell Signatures. US Patent Application US20190292606A1; 2019. doi: <https://patents.google.com/patent/US20190292606A1/en?q=US20190292606A1>.
33. Pirooznia M, Yang JY, Yang MQ, Deng Y. A comparative study of different machine learning methods on microarray gene expression data. *BMC Genomics [Electronic Resource]* 2008;9:S13.
34. Hendry S, Salgado R, Gevaert T, Russell PA, John T, Thapa B, et al. Assessing tumor-infiltrating lymphocytes in solid tumors: a practical review for pathologists and proposal for a standardized method from the international immunooncology biomarkers working group: Part 1: Assessing the host immune response, TILs in invasive breast carcinoma and ductal carcinoma in situ, metastatic tumor deposits and areas for further research. *Adv Anat Pathol* 2017;24:235–51.
35. Salgado R, Denkert C, Demaria S, Sirtaine N, Klauschen F, Pruneri G, et al. The evaluation of tumor-infiltrating lymphocytes (TILs) in breast cancer: recommendations by an International TILs Working Group 2014. *Ann Oncol* 2015;26:259–71.
36. Kather JN, Suarez-Carmona M, Charoentong P, Weis C-A, Hirsch D, Bankhead P, et al. Topography of cancer-associated immune cells in human solid tumors. *Elife* 2018;7:e36967.
37. Romero-Cordoba, Meneghini, Sant, Iorio, Sfondrini, Paolini, et al. Decoding immune heterogeneity of triple negative breast cancer and its association with systemic inflammation. *Cancers* 2019;11:911–31.
38. Rosenthal R, Cadieux EL, Salgado R, Bakir MA, Moore DA, Hiley CT, et al. Neoantigen-directed immune escape in lung cancer evolution. *Nature* 2019;567:479–85.
39. Oshi M, Asaoka M, Tokumaru Y, Angarita FA, Yan L, Matsuyama R, et al. Abundance of regulatory T cell (Treg) as a predictive biomarker for neoadjuvant chemotherapy in triple-negative breast cancer. *Cancers* 2020;12:3038.